22nd International Congress of Mechanical Engineering (COBEM 2013)
November 3-7, 2013, Ribeirão Preto, SP, Brazil

NUMERICAL ACCURACY ANALYSIS OF A GAS TURBINE HEAT TRANSFER STUDY

Grazieli Luiza Costa Carosio
Marcio Teixeira de Mendonça
Departamento de Ciência e Tecnologia Aeroespacial, Instituto de Aeronáutica e Espaço, São José dos Campos, São Paulo, 12228-904
grazieliglcc@iae.cta.br, marciomtm@iae.cta.br

Abstract. *This work focus on convection cooling at the blade trailing edge. In a previous study, a configuration consisting of plate fins as heat transfer enhancement device on turbine blade trailing edges cooling was compared with the classic circular pin fin configuration. Results of this comparison showed that the separation bubbles and the turbulence generation behind the pins are much larger than that on the plates. Therefore, the resulting pressure loss on the pin fin configuration is higher than that on the plate fin configuration when less than five plates are used. Regarding the total heat transfer, the plate fin configuration is better when more than three plates are used. The use of plates instead of pins may be a promising technique to achieve greater heat transfer and lower pressure drop. Given this context and aiming at improved accuracy and reliability, this work presents a grid dependency study in order to verify the grid quality and suitability to represent the physical phenomena of the configurations described above. The main grid controlling parameters are the grid density, grid stretching and nondimensional wall distance y^+. The result of this study shows that grid used for each configuration presented satisfactory performance.*

Keywords: *gas turbine cooling, convective cooling, computational fluid dynamic, grid dependence, numerical methods*

1. INTRODUCTION

Modern gas turbines rely on high temperature and high pressure in order to improve performance. In order to withstand these operating conditions blade cooling is needed and different cooling strategies are employed. The cooling air is usually either used in film cooling or discharged trough the trailing edge. In order to enhance heat transfer usually pins fins and other means are used to increase turbulence levels, which as a consequence results also in higher pressure drop through the passages.

Previous studies on turbine blade convective cooling present heat transfer and pressure loss characteristics of different cooling arrangements using circular pin fins (Fossen, 1982; Simoneau and Fossen, 1984; Lau *et al.*, 1989; Ligrani and Mahmood, 2003; Won *et al.*, 2004). Armstrong and Winstanley (1988) presented a review of heat transfer and pressure loss data for staggered arrays of circular pin fins in turbine cooling applications. A comparison of the various heat transfer augmentation techniques used in internal coolant passages, including pin fins, was performed by Ligrani *et al.* (2003). Different pin fin shapes and concepts have been studied as alternatives to circular fin, for example, cube- and diamond-shaped pin fins (Chyu *et al.*, 1998), elliptical pin fins (Uzol and Camci, 2005) and partial pins (Arora and Abdel-Messeh, 1989; Chi *et al.*, 2011).

In Chyu *et al.* (1998) cube- and diamond-shaped pins were used to enhance heat transfer coefficient from a surface. The authors measured mass transfer from a naphthalene surface and used the mass/heat transfer analogy to infer heat transfer results. The general trend of mass transfer enhancement does not change by changing the shape of the pins. There is an initial increase in mass transfer coefficient with increasing row number, and then the mass transfer coefficient subsides to its fully developed value. In general, cube-shaped pins show higher mass transfer coefficients near the inlet than that with diamond pins. It also shows that the cube-shaped pins have the highest mass transfer coefficients among the shapes considered; round pins have the lowest mass transfer coefficients. Corresponding pressure loss coefficients are higher for the cube and diamond shaped pins relative to the circular pins.

Results of an experimental investigation on the endwall heat transfer enhancement, total pressure loss, and wake flow field characteristics of circular and elliptical pin fin arrays were presented in Uzol and Camci (2005). Differences between the local enhancement patterns of the circular and elliptical pin fin arrays were observed. The elliptical fins have a weaker Reynolds number dependency compared to the circular pin fins, possibly due to boundary layer and separation characteristics. It was determined that, in terms of heat transfer enhancement performance, the elliptical fins not only have a lower performance compared to the circular fins, but also seem to be the least effective device among some of the other pin fin shapes that have been investigated by previous researchers.

The effect of half pins on the heat-transfer coefficient was studied in Arora and Abdel-Messeh (1989). The friction factor for different geometries of partial pins is lower for partial pins compared to full-length pins. The overall surface Nusselt numbers for different configurations were compared, showing that, in general, heat-transfer coefficient decreases when partial pins are used.

A investigation heat transfer enhancement fins composed of staggered arrays of short plates were proposed to substitute

the usual pin-fin configuration in Carosio and Mendonça (2012). The proposed configuration resulted in lower pressure drop across the length of the trailing edge region. The results revealed that a better thermal and hydrodynamic performance can be obtained with the proposed configuration. A greater number of plates was necessary to achieve the same or higher cooling rates that were achieved when using pin fins. However, even with a grater number of plate fins a lower pressure drop was achieved. The proposed configuration allowed a higher cooling with a smaller pumping power, therefore lower losses through the cooling system. Besides heat transfer, details of the flow field including turbulence parameters were discussed in order to elucidate the characteristics of the problem.

Given this context and aiming at improved accuracy and reliability, this work presents a grid dependency study in order to verify the grid quality and suitability to represent the physical phenomena of the configurations described in Carosio and Mendonça (2012). The main grid controlling parameters are the grid density, grid stretching and nondimensional wall distance y^+. Details of this methodology can be seen below. This paper is organized as follows: description of the problem, methodology, results and conclusions.

2. DESCRIPTION OF THE PROBLEM

The research presented in this paper was performed using an open source C++ collection of libraries for computational fluid dynamics (OpenFOAM[1]). The compressible Navier-Stokes equations are solved numerically based on a cell centered unstructured finite volume scheme. The turbulent stress terms were closed using a two equation turbulence model based on the Boussinesq turbulent viscosity hypothesis.

The SST (Shear Stress Transport) two equations turbulence model, originally developed by Menter (1994), is a turbulent viscosity model which uses the $k-\omega$ formulation in the inner region of the boundary layer and switches to the $k-\epsilon$ formulation in the outer region. Comparisons of various turbulence models applied to problems of heat transfer in gas turbines presented by Mangani and Bianchini (2007); Mangani *et al.* (2007) showed that the SST model is appropriate to the problem studied in this paper and its performance is superior to other two equation models in flows with adverse pressure gradient and separation zones. Thus, the SST model is used in all the simulations.

The solution methodology is based on a segregated, compressible version, pressure based SIMPLEC algorithm and a steady state solver. An algebraic multigrid solver with preconditioning is used for pressure and velocity coupling whereas a preconditioned, bi-conjugate gradient solver is used for the turbulent quantities and the energy equation. The vector field is interpolated using a Gauss linear schemes or a combination of Gauss linear scheme and first order Gauss upwind scheme.

The experiments were performed on an Intel i7 2600, 3.4Ghz, processor with 16GB of RAM, under Ubuntu Linux 12.10 64bits.

The study considers a model problem where cooling air flows through a channel with circular pin fins or plates as shown in Figs. 1 to 3. These models problem, detailed in the following, are based on the study presented by Tchatchouang *et al.* (2012); Carosio and Mendonça (2012).

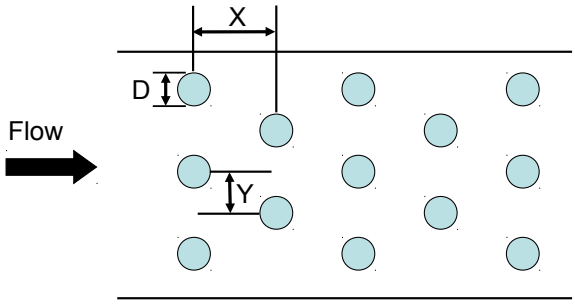

Figure 1. Circular pin fin cooling configuration.

Specifically, the circular pin diameter is $D = 6.35 \times 10^{-3}$ m, the plate thickness is $d = 0.1D = 0.635 \times 10^{-4}$ m, the plate length is $L = D$ and the channel height is $H = 4D = 25.4 \times 10^{-3}$ m. The longitudinal horizontal spacing between pins (or plates) is $X = 2.5D$. A straight channel $4X = 10D$ long is used upstream of the pin fin/plate region in order to allow the flow to develop from the inlet boundary condition. The pin fin/plate region channel length is $10X = 25D$ and the spanwise spacing is $Y = 1.25D$. At the exit a straight channel with length $4X = 10D$ is used to avoid outflow boundary condition effects on the domain of interest. The pin fin/plate section has 10 rows of staggered pin fin/plates. In the spanwise direction a symmetry condition is imposed and a larger number of plates is simulated by reducing the spanwise domain.

The air enters the inlet of the computational domain with a uniform temperature of 343.15 K and uniform velocity of

[1] http://www.openfoam.com/

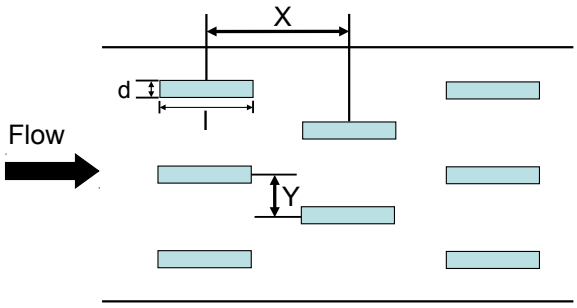

Figure 2. Plates cooling configuration.

8.24 m/s. A fixed temperature of 313.15 K is imposed on the walls. At the exit a pressure level of 101320 Pa is imposed. Turbulence parameters are imposed at the inlet corresponding to a turbulence level of 30%. This level was adjusted for comparison with results of Tchatchouang *et al.* (2012) whose turbulence parameters were not reported.

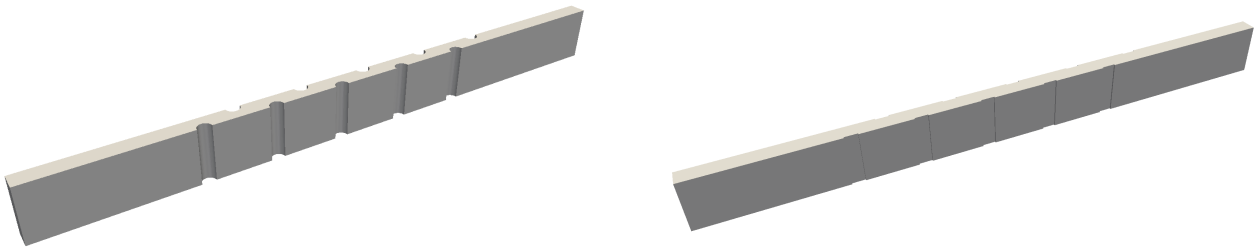

Figure 3. Computational domains.

3. METHODOLOGY

A grid sensitivity study was performed to verify the computational model for each configuration. The grid is generated using blockMesh, a grid generator available in OpenFOAM. All cells are composed of hexahedral volumes. The computational grids are shown in Fig. 4.

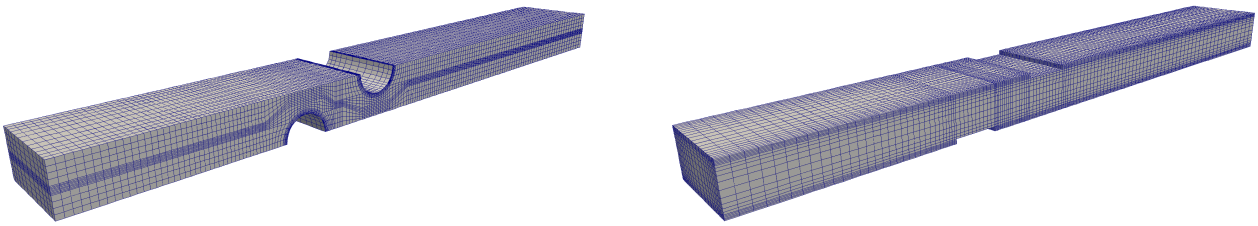

Figure 4. Computational grids.

The evaluation of the discretization errors from the computational model is performed by the study of grid dependence conducted according to the Grid Convergence Index (GCI) (ASME, 2009; Oberkampf and Trucano, 2002). This method is based on Richardson extrapolation and its basic idea is to approximately relate the results from any grid convergence test to the expected results from a grid doubling using a 2nd-order method (Roache, 1998).

In GCI, uncertainties associated with grid convergence are quantified and a bandwidth of the difference between the computed value and the asymptotic value is provided. The solution is in the asymptotic region when we obtain small values of this index. The equation to obtain such index is given below.

$$GCI_{21} = Fs\frac{\left|\frac{\phi_1-\phi_2}{\phi_1}\right|}{(r_{21}^p-1)}, \tag{1}$$

where F_s is the safety factor that is equal to 1.25 for three grids (Roache, 1998), ϕ_1 and ϕ_2 are solutions of the fine and coarse grids respectively, r is grid refinement factor, and p is observed order of the scheme.

Given that the grids used are not structured, r is calculated according to the eq. 2.

$$r = \left(\frac{N1}{N2}\right)^{D}, \tag{2}$$

where $N1$ and $N2$ are the fine and coarse grid cells number, and D is the dimension of the model. In Celik *et al.* (2008), r is recommended to be greater than 1.3. For the grids used r is greater than 1.36 in all the cases studied in this paper.

Since r is not constant between grids, we will use eq. 3 to calculate p.

$$p = \frac{1}{\ln(r_{21})}\left|\ln\left|\frac{\phi_3-\phi_2}{\phi_2-\phi_1}\right| + \ln\left(\frac{r_{21}^{p} - sgn\left(\frac{\phi_3-\phi_2}{\phi_2-\phi_1}\right)}{r_{32}^{p} - sgn\left(\frac{\phi_3-\phi_2}{\phi_2-\phi_1}\right)}\right)\right|, \tag{3}$$

where sgn(x) is signal function defined by

$$sgn(x) = \begin{cases} -1 & \text{if } x < 0 \\ 0 & \text{if } x = 0 \\ 1 & \text{if } x > 0 \end{cases}$$

Remember that the theoretical order is equal to 2 for the finite volume method.

4. RESULTS

Results of the grid dependence study and validation of the code are presented on this section. The verification is performed by the study of grid dependence conducted according to the verification methodology proposed by Roache (1998) — the Grid Convergence Index (GCI). Regarding the validation, CFD generated results were compared with numerical results of Tchatchouang *et al.* (2012); Chi *et al.* (2011) and experimental results of Siw *et al.* (2010).

4.1 Verification

Three different grid densities for the circular pin fin configuration were considered, 1,660,512 grid cells, 490,560 grid cells, and 142,296 grid cells. Table 1 shows a grid dependency study in terms of temperature (T) in Kelvin, pressure drop (dp) in Pascal, heat flux (q) in Watt and non-dimensional wall distance (y^+). The grid dependence study used a domain with only two pin fins in the longitudinal direction. To generate the domain with ten pin fins Tchatchouang *et al.* (2012) the same grid was used for each block of two pins. The grid dependence study was done in this way to reduce computational cost.

Table 2 shows a similar grid dependency study, but considering the configuration with plates. The following grid densities where considered: 953,712; 372,192; and 145,216.

Again, the grid dependence study used a domain with two rows of plates and the same grid was used for each block of two plates to create a domain with ten plates.

Table 1. Grid dependency test. Circular pin fins.

	T (K)	dp (Pa)	q (W)	y^+
grid 1	338.9	70	6.83	0.92
grid 2	338.9	68	6.82	0.98
grid 3	338.8	63	6.71	1.04

Tables 1 and 2 show that the adjustment of the parameters - grid density and grid stretching - enabled a y^+ value close to 1. Tables 3 and 4 show the temperature (T) in Kelvin, the order p, the percentage of the relative error (ϵ) and the GCI for three positions specified.

In addition to the positions of Table 3 the order p for another 37 positions were calculated. The range for p is from 0.026 to 9.339; the average p is equal to 2.342; and the average GCI_{12} is equal to the average GCI_{23}, that is 1.2×10^{-2}.

Besides the temperature, other properties were considered to calculate the order p such as turbulent kinetic energy, velocity and pressure. Considering the turbulent kinetic energy, the range for p is from 0.045 to 5.436; the average p is

Table 2. Grid dependency test. Plate fins.

	T (K)	dp (Pa)	q (W)	y^+
grid 1	339.67	12.45	4.96	1.05
grid 2	339.63	12.55	4.96	0.99
grid 3	339.58	12.68	4.85	0.98

Table 3. GCI. Circular pin fins.

Position (m)		T(K)			order p	ϵ %	GCI %
x	y	Grid 1	Grid 2	Grid 3			
0.079	0.004	342.14	342.06	341.98	0.22	2.4e-04	4.2e-03
0.090	0.005	334.63	334.67	336.66	9.34	1.3e-04	3.4e-06
0.095	0.008	337.76	337.82	338.07	4.39	1.9e-04	7.8e-05

Table 4. GCI. Plate fins.

Position (m)		T(K)			order p	ϵ %	GCI %
x	y	Grid 1	Grid 2	Grid 3			
0.079	0.004	343.08	342.99	342.88	0.55	2.6e-04	2.4e-03
0.095	0.007	338.58	338.76	338.82	3.10	5.3e-04	3.8e-04
0.095	0.008	337.15	336.77	336.64	3.50	1.1e-03	7.1e-04

equal to 2.144; the average GCI_{12} is equal to 0.142, and the average GCI_{23} is 0.165. In turn, considering the velocity, the range for p is from 0.204 to 8.762; thye average p is equal to 1.651; the average GCI_{12} is equal to the average GCI_{23} that is 0.26. Finally, considering the pressure, the range for p is from 0.334 to 5.235; the average p is equal to 1.825; the average GCI_{12} is equal to 3.9×10^{-5}, and the average GCI_{23} is 5.4×10^{-5}.

According to the results presented above, we conclude that the GCI values are close to zero and the average observed order is close to the theoretical order, confirming the quality of the grid. Future simulations will be performed with the second grid size because this grid is not very coarse nor very fine and presented satisfactory results.

Similarly, in addition to the positions of Tab. 4 the p value for another 29 positions were calculated. The range for p is from 0.011 to 8.715; the average p is equal to 2.003; and the average GCI_{12} is equal to the average GCI_{23} that is 3.2×10^{-3}.

Besides the temperature, other properties were considered for the evaluation of p such as turbulent kinetic energy, velocity, and pressure. Considering the turbulent kinetic energy, the range for p is from 0.05 to 10.464; the average p is equal to 1.57; the average GCI_{12} is equal to 8.178, and the average GCI_{23} is 4.848. In turn, considering the velocity, the range for p is from 0.011 to 3.456; the average p is equal to 1.414; the average GCI_{12} is equal to 0.192, and the average GCI_{23} is 0.161. Finally, considering the pressure, the range for p is from 0.014 to 10.204; the average p is equal to 2.258; the average GCI_{12} is equal to the average GCI_{23} that is 4.4×10^{-5}.

According to the results presented above, we conclude that the GCI values are close to zero for the temperature and pressure. Accordingly, the average observed order is close to the theoretical order only for pressure and temperature. Considering the turbulent kinetic energy and velocity, the results indicate that it is still necessary to make some adjustments in the grid in order to enhance the grid quality. The positions where the results are worse are been evaluated and further grid refinement in these particular positions will improve the average order p and GCI values.

4.2 Validation

To validate the setup, CFD generated results were compared with numerical results from Tchatchouang *et al.* (2012) and Chi *et al.* (2011), and experimental results from Siw *et al.* (2010). Figure 5 shows the comparison considering the zonally averaged convection heat transfer coefficient h. From this figure, it can be seen that the zonally-averaged h computed by CFD is considerably lower than the experimentally-measured zonally-averaged h. The numerical results from Tchatchouang *et al.* (2012) and Chi *et al.* (2011) show similar differences to the experimental results and they state that the measurements based on transient liquid crystal (TLC) technique does not compare well with the steady state CFD analysis that uses isothermal walls. The error can be as high as 50% for the circular pin fins. Considering this and that the general behavior of h along the channel was well reproduced and match the numerical results of Tchatchouang *et al.* (2012) and Chi *et al.* (2011), the validation presented in Fig. 5 is consistent.

Armstrong and Winstanley (1988) compared different correlations with available experimental data and observed that the difference between correlations and experiments can be of the order of plus or minus 20%. The averaged Nusselt number obtained in the present CFD simulation was compared to the average Nusselt number given by one of Metzger's correlations ($Nu = 0.069Re^{0.728}$, (Moores, 2008)). The Reynolds number reference velocity is the velocity at the minimum area between pins and the reference length is the pin fin diameter. For the parameters considered, the correlation gives $Nu = 39.86$ while de CFD gives $Nu = 38.97$, which results in a difference of 2.24%.

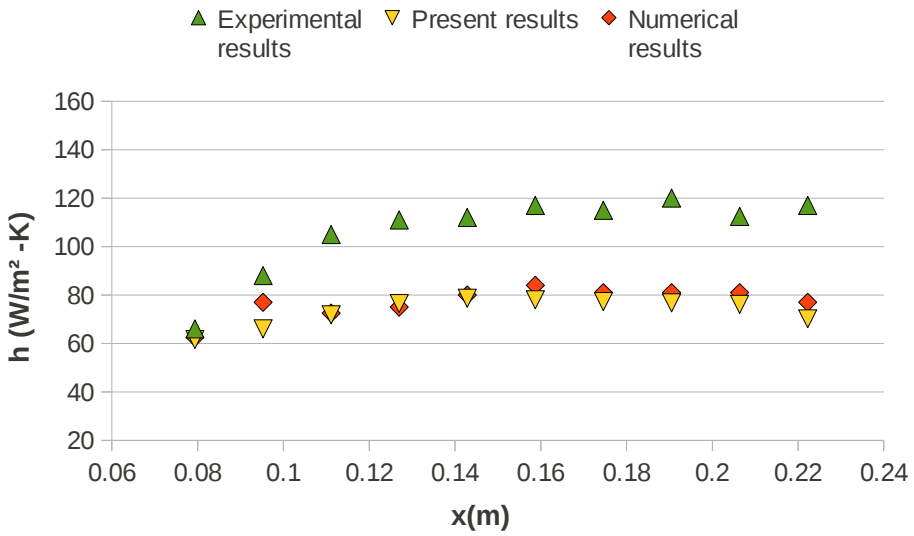

Figure 5. Averaged heat transfer coefficient.

5. CONCLUSIONS

This work presents a grid dependency study in order to verify the grid quality and suitability to represent the physics of the circular pin fins and plate fins configurations. The main grid controlling parameters are the grid density, grid stretching and nondimensional wall distance y^+. For all cases studied, the grid density and grid stretching were adjusted to ensure that y^+ was around 1. We obtained small values of the GCI for all properties considered - temperature, turbulent kinetic energy, velocity, and pressure - confirming that the solution is in the asymptotic region. Besides the average order p was around 2, i.e., the observed order was close to a theoretical order of the method. The result of this study showed that grid used for pin configuration presented satisfactory performance. Regarding the plate configuration, small values of the GCI were obtained and the average observed order was close to the theoretical order only when pressure and temperature were considered. Therefore, the grid used for the plate configuration needs some adjustments to improve quality and to obtain small values of the GCI for all properties considered.

6. ACKNOWLEDGEMENTS

The authors would like acknowledge the support from National Counsel of Technological and Scientific Development (CNPq) and from State of São Paulo Research Foundation (FAPESP).

7. REFERENCES

Armstrong, J. and Winstanley, D., 1988. "A review of staggered array pin fin heat transfer for turbine cooling applications". *ASME J. Turbomach.*, Vol. 110, pp. 94–103.

Arora, S.C. and Abdel-Messeh, W., 1989. "Characteristics of partial length circular pin fins as heat transfer augmentors for airfoil internal cooling passages". In *Gas Turbine and Aeroengine Congress and Exposition*. ASME, Toronto, Canada. ASME Paper No. 89-GT-87.

ASME, 2009. *Standard for Verification and Validation in Computational Fluid Dynamics and Heat Transfer*. ASME V&V 20-2009. American Society of Mechanical Engineers, New York.

Carosio, G.L.C. and Mendonça, M.T., 2012. "Comparative analysis of turbine blade trailing edge cooling configurations". In *Proceedings of the 14th ENCIT*. In: 14th Brazilian Congress of Thermal Sciences, Associação Brasileira de Engenharia e Ciências Mecânicas–ABCM, Rio de Janeiro.

Celik, I.B., Ghia, U., Roache, P.J., Freitas, C.J., Coleman, H. and Raad, P.E., 2008. "Procedure for estimation and reporting of uncertainly due to discretization in cfd applications". *ASME Journal of Fluids Engineering*, Vol. 130, pp.

078001–1–078001–4.

Chi, X., Shih, T.P., Bryden, K.M., Siw, S., Chyu, M.K., Ames, R. and Dennis, R.A., 2011. "Effects of pin-fin height on flow and heat transfer in a rectangular duct". In *Proceedings of ASME Turbo Expo 2011*. ASME, Vancouver, Canada. ASME Paper No. GT2011-46014.

Chyu, M.K., Hsing, Y.C. and Natarajan, V., 1998. "Convective heat transfer of cubic fin arrays in a narrow channel". *ASME Journal of Turbomachinery*, Vol. 120, pp. 362–367.

Fossen, G.J.V., 1982. "Heat transfer coefficients for staggered arrays of short pin fins". *ASME J. Eng. Power*, Vol. 104, pp. 268–284.

Lau, S.C., Han, J.C. and Batten, T., 1989. "Heat transfer, pressure drop and mass-flow rate in pin fin channels with long and short trailing edge ejection holes". *ASME J. Turbomach.*, Vol. 111, pp. 116–123.

Ligrani, P.M. and Mahmood, G.I., 2003. "Variable property nusselt numbers in a channel with pin-fins". *AIAA J. Thermophys. Heat Transfer*, Vol. **v. 17**, pp. 103–111.

Ligrani, P.M., Oliveira, M.M. and Blaskovich, T., 2003. "Comparison of heat transfer augmentation techniques". *AIAA Journal*, Vol. **v. 41**, No. 3, pp. 337–362.

Mangani, L. and Bianchini, C., 2007. "Heat transfer applications in turbomachinery". In *Proceedings of the OpenFOAM International Conference*. OpenFOAM Conference, London, Reino Unido.

Mangani, L., Bianchini, C., Andreini, A. and Facchini, B., 2007. "Development and validation of a c++ object oriented cfd code for heat transfer analysis". In *Proceedings of the ASME-JSME Thermal Engineering Conference and Summer Heat Transfer Conference*. ASME, Vancouver, Canada. ASME Paper No. 2007-AJ-1266.

Menter, F.R., 1994. "Two-equation eddy-viscosity turbulence models for engineering applications". *AIAA Journal*, Vol. **v. 32**, No. 8, pp. 1598–1605.

Moores, K.A., 2008. *Effect of Tip Clearance on the Thermal and Hydrodynamic Performance of Shrouded Pin Fin Arrays*. Ph.D. thesis, University of Maryland, College Park, MD.

Oberkampf, W.L. and Trucano, T.G., 2002. "Verification and validation in computational fluid dynamics". Technical report, Sandia National Laboratories, Albuquerque, New Mexico.

Roache, P., 1998. *Fundamentals of Computational Fluid Dynamics*. Hermosa Publishers.

Simoneau, R.J. and Fossen, G.J.V., 1984. "Effect of location in an array on heat transfer to a short cylinder in crossflow". *ASME J. Heat Transfer*, Vol. 106, pp. 42–48.

Siw, S.C., Chyu, M.K., Shih, T.P. and Alvin, M.A., 2010. "Effects of pin detached space on heat transfer in fin arrays". In *Proceedings of ASME Turbo Expo 2010*. ASME, Glasgow, Scotland. ASME Paper No. GT2010-23227.

Tchatchouang, C.W., Chi, X., Shih, T.P., Bryden, K.M., Ames, R. and Dennis, R.A., 2012. "Effects of turbulence modeling in predicting flow and heat transfer in a duct with pin fins". In *Proceedings of AIAA Turbo Expo 2011*. AIAA, Nashville, United States. AIAA Paper No. 2012-0527.

Uzol, O. and Camci, C., 2005. "Heat transfer, pressure loss and flow field measurements downstream of staggered two-row circular and elliptical pin fin arrays". *ASME Journal of Heat Transfer*, Vol. 127, No. 5, pp. 458–471.

Won, S.Y., Mahmood, G.I. and Ligrani, P.M., 2004. "Spatially-resolved heat transfer and flow structure in a rectangular channel with pin-fins". *Int. J. Heat Mass Transfer*, Vol. **v. 47**, pp. 1731–1743.

8. RESPONSIBILITY NOTICE

The authors are the only responsible for the printed material included in this paper.